

# Harnessing Sparsity over the Continuum: Atomic Norm Minimization for Super Resolution

Yuejie Chi, *Senior Member, IEEE*, Maxime Ferreira Da Costa, *Member, IEEE*

At the core of many sensing and imaging applications, the signal of interest can be modeled as a linear superposition of translated or modulated versions of some template (e.g. a point spread function, a Green's function), and the fundamental problem is to estimate the translation or modulation parameters (e.g. delays, locations, Dopplers) from noisy measurements. This problem is of central importance to not only target localization in radar and sonar, channel estimation in wireless communications, direction-of-arrival estimation in array signal processing, but also modern imaging modalities such as super-resolution single-molecule fluorescence microscopy, nuclear magnetic resonance imaging, spike localization in neural recordings, among others.

Typically, the temporal or spatial resolution of the acquired signal is limited by that of the sensing or imaging devices, due to factors such as the numerical aperture of a microscopy, the wavelength of the impinging electromagnetic or optical waves, or the sampling rate of an analog-to-digital converter. This resolution limit is well-known and often referred to as the *Rayleigh limit* (c.f. the box “What is the Rayleigh Limit?”). The performance of matched filtering, or periodogram, which creates a correlation map of the acquired signal against the range of parameters, is limited by the Rayleigh limit, regardless of the noise level.

On the other hand, the desired resolution of parameter estimation can be much higher – a challenge known as *super resolution*. There is a long history of pursuing super-resolution algorithms in the community of signal processing [1], [2]. The oldest one probably dates back to de Prony's root finding method in as early as 1795 [3], and variants of this method that are better suited for noisy data have also been proposed over time [4]. Subspace methods based on the computation of eigenvector or singular vector decompositions, such as MUSIC [5], ESPRIT [6] and matrix pencil [7], are another class of popular approaches since their inception in 1980s. Different forms of maximum likelihood estimators [8], [9] have also been studied extensively. Collectively, these algorithms have “super resolution” capabilities, namely, they can resolve the parameters of interest at a resolution below the Rayleigh limit when the noise level is sufficiently small.

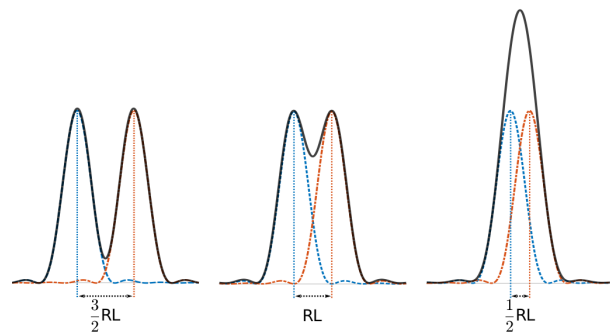
While there already exists a plethora of traditional methods, convex optimization recently emerges as a compelling framework for performing super resolution, garnering significant

The authors are with the Department of Electrical and Computer Engineering, Carnegie Mellon University, Pittsburgh, PA, USA (emails: {yuejiechi, mferreira}@cmu.edu).

This work is supported in part by ONR under grant N00014-18-1-2142, and by NSF under grants CIF-1826519 and ECCS-1818571.

## What is the Rayleigh Limit?

The Rayleigh limit is an *empirical* criterion characterizing the resolution of an optical system due to diffraction. Taking a conventional fluorescence microscopy as an example, the observed diffraction patterns of two fluorescent point sources become visually harder to distinguish as the point sources get closer to each other, illustrated below. We say they are no longer resolvable when their separation is below the Rayleigh limit (RL). In this context, the RL is given as  $1.22\lambda/\text{NA}$  [10], where  $\lambda$  is the wavelength of the emission light, and NA is the numerical aperture of the objective lens. The constant 1.22 is related to the roots of Bessel functions of the first kind used to model the point spread function, and can vary for different setups.



attention from multiple communities spanning signal processing, applied mathematics, and optimization. Due to (the relative) tractability of convex analysis and convex optimization, the new framework offers several benefits. First, strong theoretical guarantees are rigorously established to back up its performance even in the presence of noise and corruptions. Second, it is versatile to include prior knowledge into the convex program to handle a wide range of measurement models that fall out of the reach of traditional methods. Third, leveraging the rapid progress in large-scale convex optimization, it opens up the possibility of applying efficient tailored solvers for real-world applications.

The goal of this paper is to offer a friendly exposition to atomic norm minimization [11] as a *canonical* convex approach for super resolution, highlighting its mathematical formulation and application in super resolution image reconstruction for single-molecule fluorescence microscopy [12]. The atomic norm is first proposed in [13] as a general framework for designing tight convex relaxations to promote “simple” signal decompositions, where one seeks to use a minimal number of

“atoms” to represent a given signal from an atomic set composed of an ensemble of signal atoms. Celebrated convex relaxations such as the  $\ell_1$  norm approach for cardinality minimization [14] and the nuclear norm approach for rank minimization [15] can be viewed as particular instances of atomic norms for appropriately defined atomic sets. Specializing the atomic set to a dictionary containing all translations of the template signal over the continuous-valued parameter space, estimating the underlying translation parameters is then equivalent to identifying a sparse decomposition in an infinite-dimensional dictionary. This key observation allows one to recast super resolution as solving an infinite-dimensional convex program [16] – a special form of atomic norm minimization considered in this paper.

Throughout this paper, we use boldface letters to represent matrices and vectors, e.g.  $\mathbf{a}$  and  $\mathbf{A}$ . We use  $\mathbf{A}^\top$ ,  $\mathbf{A}^H$ ,  $\text{Tr}(\mathbf{A})$  to represent the transpose, Hermitian transpose, and trace of  $\mathbf{A}$ , respectively. We use  $\mathbf{A} \succeq 0$  to represent  $\mathbf{A}$  is positive semidefinite. The matrix  $\text{toep}(\mathbf{u})$  denotes the Hermitian Toeplitz matrix whose first column is equal to  $\mathbf{u}$ , and  $\text{diag}(\mathbf{g})$  denotes the diagonal matrix with diagonal entries given as  $\mathbf{g}$ . Define by  $\langle \mathbf{X}, \mathbf{P} \rangle = \text{Tr}(\mathbf{X}^H \mathbf{P})$  the inner product between two matrices  $\mathbf{X}$  and  $\mathbf{P}$ . The indicator function  $\delta_k$  equals to 1 if  $k = 0$  and 0 otherwise. Additionally, the notation  $f(n) = O(g(n))$  means that there exists a constant  $c > 0$  such that  $|f(n)| \leq c|g(n)|$ .

## I. WHAT IS THE ATOMIC NORM?

An everlasting idea in signal processing is decomposing a signal into a linear combination of judiciously chosen basis vectors, and seeking compact and interpretable signal representations that are useful for downstream processing. For example, decomposing time series into sinusoids, speeches and images into wavelets, total system responses into impulse responses, etc.

To fix ideas, consider the task of representing a signal  $\mathbf{x}$  in a vector space using *atoms* from a collection of vectors in  $\mathcal{A} = \{\mathbf{a}_i\}$  called an *atomic set*. The set  $\mathcal{A}$  can contain either finite or infinite numbers of atoms. We wish to expand  $\mathbf{x}$  using the atoms in a form of

$$\mathbf{x} = \sum_i c_i \mathbf{a}_i, \quad \mathbf{a}_i \in \mathcal{A}, \quad (1)$$

where  $c_i > 0$  specifies the coefficients of the decomposition. In many applications, the size of  $\mathcal{A}$  can be much larger than the dimension of the signal, leading to an overcomplete representation, and there are an infinite number of possibilities to decompose  $\mathbf{x}$ . Which representation shall we pick? Among the many plausible criteria, one meaningful approach is to pursue the Occam’s razor principle, and seek for a parsimonious decomposition of the signal  $\mathbf{x}$  involving the *smallest possible number of atoms* in  $\mathcal{A}$ , i.e. the sparsest solution to (1). The corresponding representation is known as a *sparse representation* [17]. Many real-world signals admit sparse representations for appropriately chosen atomic sets. As a simple example, natural images are approximately sparse by picking  $\mathcal{A}$  as a wavelet frame. Low-rank matrices, another class of signals possessing low-dimensional structures that have enjoyed wide success in

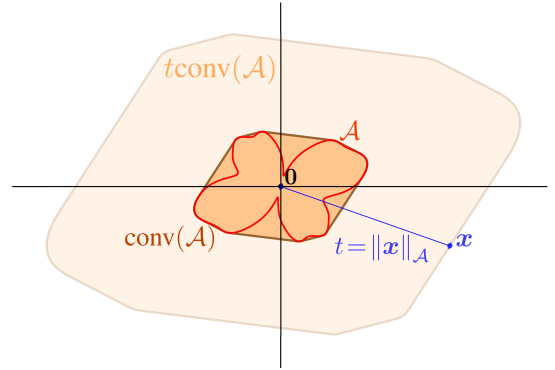


Fig. 1. An atomic set  $\mathcal{A}$  (in red) and its convex hull  $\text{conv}(\mathcal{A})$  (in orange). The atomic norm of a vector  $\mathbf{x}$  can be interpreted as the smallest dilation factor  $t \geq 0$  such that  $\mathbf{x}$  belongs to  $t \text{conv}(\mathcal{A})$  (in blue).

signal processing [18], are sparse with respect to an atomic set  $\mathcal{A}$  that is the collection of all rank-one matrices.

Given a signal  $\mathbf{x}$  and an atomic set  $\mathcal{A}$ , how to find its sparse representation? In general, this problem is nonconvex and can be NP-hard due to the combinatorial aspect of cardinality minimization. The key motivation behind atomic norm minimization, proposed by Chandrasekaran et. al. [13], is to relax the nonconvex sparsity cost by its tight convex surrogate, and solve instead the resulting convex relaxation that is more tractable. This idea is a generalization of the popular  $\ell_1$  minimization for sparse vector recovery [19], [20] when  $\mathcal{A}$  is a *finite* set. Therein, one seeks to solve a linear program which minimizes the sum instead of the cardinality of the nonzero coefficients.

To extend the same idea to the case where  $\mathcal{A}$  is an arbitrary, and possibly infinite-dimensional set, we first take the convex hull of  $\mathcal{A}$ , denoted as  $\text{conv}(\mathcal{A})$ , and then define its associated Minkowski functional (or gauge function) as [13]

$$\|\mathbf{x}\|_{\mathcal{A}} \triangleq \inf \{t \geq 0 : \mathbf{x} \in t \text{conv}(\mathcal{A})\}, \quad (2)$$

which is the infimum of a convex program. When  $\mathcal{A}$  is centrally symmetric about the origin, the above definition leads to a valid norm, and is called the *atomic norm* of  $\mathbf{x}$ . Fig. 1 presents an illustration of this concept, where the atomic norm is the smallest nonnegative scaling of  $\text{conv}(\mathcal{A})$  until it intersects  $\mathbf{x}$ . Following the definition (2), a fundamental geometric property is that the atomic norm ball, i.e.,  $\{\mathbf{x} : \|\mathbf{x}\|_{\mathcal{A}} \leq 1\}$ , is exactly  $\text{conv}(\mathcal{A})$ .

More interestingly, consider the case when  $\mathbf{x}$  lies in an  $n$ -dimensional vector space. Carathéodory’s theorem [21] guarantees that any point in  $\text{conv}(\mathcal{A})$  can be decomposed as a convex combination of at most  $n + 1$  points in  $\mathcal{A}$ , where  $\mathcal{A}$  is not necessarily convex. Therefore, one may rewrite (2) as

$$\|\mathbf{x}\|_{\mathcal{A}} = \inf \left\{ \sum_i c_i : \mathbf{x} = \sum_i c_i \mathbf{a}_i, c_i > 0, \mathbf{a}_i \in \mathcal{A} \right\}. \quad (3)$$

The decomposition  $\sum_i c_i \mathbf{a}_i$  that obtains the infimum is referred to as the *atomic decomposition* of  $\mathbf{x}$  onto  $\mathcal{A}$ . It is not hard to see that the atomic norm indeed subsumes the  $\ell_1$  norm as a special case but accommodates more general case where  $\mathcal{A}$

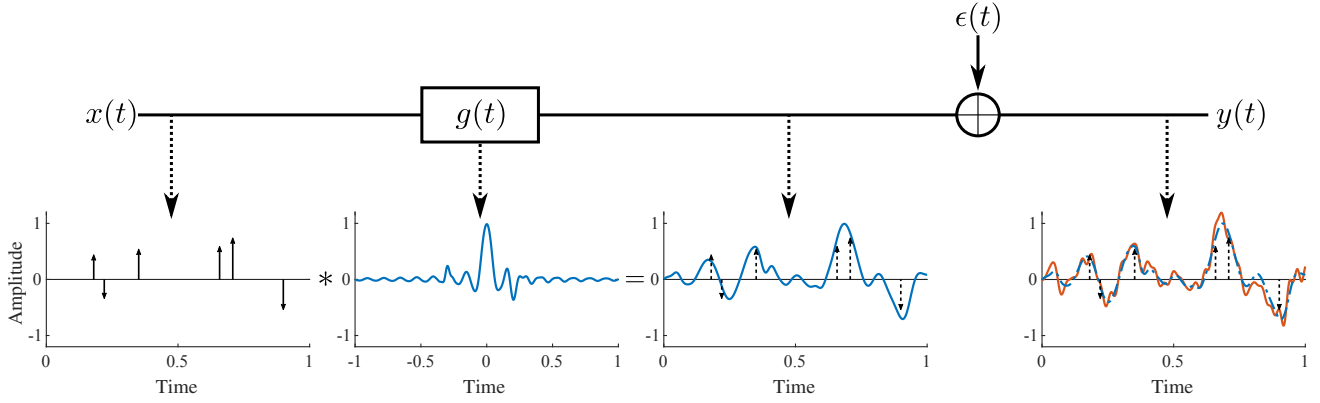


Fig. 2. An illustration of the mathematical model. The spike signal  $x(t)$  is convolved with a point spread function  $g(t)$ , leading to degradation of its resolution, which is further exacerbated by an additive noise  $\epsilon(t)$ , producing an output signal  $y(t)$ .

can be an infinite-dimensional set.

Several central questions are how to compute the atomic norm and find the atomic decomposition, and when the atomic decomposition coincides with the sparse representation, i.e. the convex relaxation is tight. These questions have been addressed extensively in the study of  $\ell_1$  minimization for sparse vector recovery [19], [20], [22]. We will address these questions in the context of super resolution.

## II. A MATHEMATICAL MODEL OF SUPER RESOLUTION

We focus on a simple yet widely applicable model for super resolution that describes the convolution of a sequence of point sources with a point spread function (PSF) that is resolution-limited, illustrated in Fig. 2. Let  $x(t)$  be a spike signal given as

$$x(t) = \sum_{k=1}^r c_k \delta(t - \tau_k). \quad (4)$$

Here,  $r$  is the number of spikes,  $c_k \in \mathbb{C}$  and  $\tau_k \in [0, 1]^1$  are the complex amplitude and delay of the  $k$ th spike. Such a spike signal can model many physical phenomena, such as firing times of neurons, locations of fluorescence molecules, and so on. Let  $g(t)$  be the PSF whose bandwidth is limited due to the Rayleigh limit, namely its Fourier transform  $G(f)$  satisfies

$$G(f) = 0 \quad \text{whenever} \quad |f| > B/2$$

for some bandwidth  $B > 0$ . Its convolution with  $x(t)$ , contaminated by an additive noise  $\epsilon(t)$ , can be written as

$$y(t) = x(t) * g(t) + \epsilon(t) = \sum_{k=1}^r c_k g(t - \tau_k) + \epsilon(t),$$

where  $*$  denotes the convolution operator. Sampling the Fourier transform of the above equation at the frequencies  $\ell = -\lfloor B/2 \rfloor, \dots, 0, \dots, \lfloor B/2 \rfloor$ , we obtain the measurements

$$Y_\ell = G_\ell \cdot X_\ell + E_\ell = G_\ell \cdot \left( \sum_{k=1}^r c_k e^{j2\pi\ell\tau_k} \right) + E_\ell, \quad (5)$$

where  $G_\ell$ ,  $X_\ell$ ,  $E_\ell$ , and  $Y_\ell$  are the Fourier transforms of  $g(t)$ ,  $x(t)$ ,  $\epsilon(t)$ , and  $y(t)$  evaluated at frequency  $\ell$ , respectively. The

<sup>1</sup>Without loss of generality, the maximal delay is normalized to 1.

total number of samples is  $n = 2\lfloor B/2 \rfloor + 1$ , proportional to the bandwidth  $B$ . We write (5) in a vector form as

$$\mathbf{y} = \text{diag}(\mathbf{g})\mathbf{x} + \boldsymbol{\epsilon}, \quad (6)$$

where  $\mathbf{y} = [Y_\ell]$ ,  $\mathbf{g} = [G_\ell]$ ,  $\mathbf{x} = [X_\ell]$ , and  $\boldsymbol{\epsilon} = [E_\ell]$ . The problem of super resolution is then to estimate  $\{c_k, \tau_k\}_{1 \leq k \leq r}$  accurately from  $\mathbf{y}$ , without knowing the model order  $r$  a priori. Here, the Rayleigh limit is inversely proportional to the bandwidth  $B$ , and roughly speaking, is about  $1/n$ .

When the PSF  $g(t)$  is known, one can “equalize” (5) by multiplying both sides by  $G_\ell^{-1}$ , provided that the  $G_\ell$ ’s are non-zero. The observation  $\mathbf{z} = [G_\ell^{-1}Y_\ell]$  relates to  $\mathbf{x}$  as

$$\mathbf{z} = \mathbf{x} + \tilde{\boldsymbol{\epsilon}}, \quad (7)$$

where  $\tilde{\boldsymbol{\epsilon}}$  is the additive noise. With slight abuse of notation, we shift the index of  $\ell$  to  $0, \dots, n-1$  for convenience, and write  $\mathbf{x}$  as a superposition of complex sinusoids:

$$\mathbf{x} = \sum_{k=1}^r c_k \mathbf{a}(\tau_k), \quad (8)$$

where  $\mathbf{a}(\tau) \in \mathbb{C}^n$  is a vector defined as

$$\mathbf{a}(\tau) = \left[ 1, e^{j2\pi\tau}, \dots, e^{j2\pi(n-1)\tau} \right]^\top, \quad \tau \in [0, 1]. \quad (9)$$

Notably, the above simplified model (7) also amounts to the classical problem of *line spectrum estimation*, that consists of estimating a mixture of sinusoids from its equi-spaced time samples. The same model can also describe direction-of-arrivals estimation using a uniform linear array, which is studied extensively in the literature of spectrum analysis [1].

## III. SUPER RESOLUTION VIA ATOMIC NORM MINIMIZATION

In the absence of noise, one could think of super resolution as estimating the continuous-time spike signal  $x(t)$  in (4) from its discrete-time moment measurements  $\mathbf{x}$  in (8), which are related through

$$\mathbf{x} = \int_0^1 \mathbf{a}(t) dx(t).$$

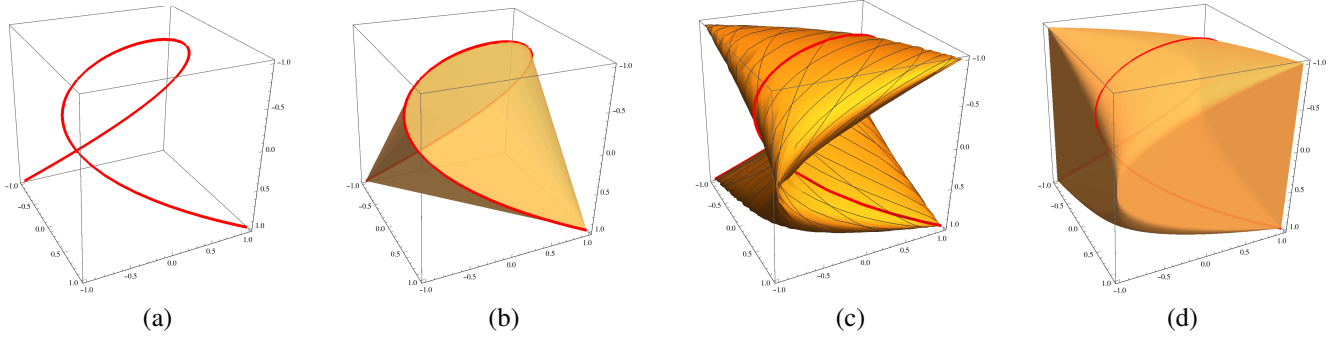


Fig. 3. Visualization of the continuous-valued atomic set for super resolution. (a) The moment curve  $\mathcal{A}_0$  restricted to the 3 real moments  $\{\cos(2\pi\tau), \cos(4\pi\tau), \cos(6\pi\tau)\}^\top : \tau \in [0, 1]\}$ , and (b) its convex hull. (c) The phased version of the moment curve  $\mathcal{A}_{1D}$  restricted to the 3 real moments  $\{\cos(2\pi\tau + \phi), \cos(4\pi\tau + \phi), \cos(6\pi\tau + \phi)\}^\top : \tau \in [0, 1], \phi \in [0, 2\pi]\}$ , and (d) its convex hull.

One can also think of  $x(t)$  as the representation of  $\mathbf{x}$  over a continuous dictionary

$$\mathcal{A}_0 = \{\mathbf{a}(\tau) : \tau \in [0, 1]\}, \quad (10)$$

which forms a one-dimensional variety of  $\mathbb{C}^n$  called the *moment curve*, illustrated in Fig. 3 (a). It is well-known that the convex hull of  $\mathcal{A}_0$ , illustrated in Fig. 3 (b), is a body of  $\mathbb{C}^n$  that can be parameterized by a set of linear matrix inequalities [23], and has close relationships with the positivity of Hermitian Toeplitz matrices. This fundamental property of the moment curve has many implications in control and signal processing [24], [25], and is key to the development of a super-resolution theory based on atomic norm minimization.

It is clearly possible to obtain the same measurements  $\mathbf{x}$  with different  $x(t)$ , however, if we impose some sparsity assumption, namely constraining how many spikes are allowed in  $x(t)$ , this representation can be ensured to be unique. In particular, the representation (8) is unique as long as  $r \leq \lfloor n/2 \rfloor$  and the support set  $\mathcal{T} = \{\tau_k\}_{1 \leq k \leq r}$  contains distinct elements.

#### A. Atomic Norm for Super Resolution

To apply the framework of atomic norm minimization for super resolution, one must first define the atomic set properly. Since the complex amplitudes  $c_k$ 's can be taken arbitrary phases, we introduce an augmented atomic set taking this into account:

$$\mathcal{A}_{1D} = \{e^{j\phi} \mathbf{a}(\tau) : \tau \in [0, 1], \phi \in [0, 2\pi]\}. \quad (11)$$

See an illustration of  $\mathcal{A}_{1D}$  and its convex hull in Fig. 3 (c) and (d). Writing  $c_k = |c_k| e^{j\phi_k}$ ,  $\mathbf{x}$  can be represented as a positive combination of the atoms in  $\mathcal{A}_{1D}$  as  $\mathbf{x} = \sum_{k=1}^r |c_k| e^{j\phi_k} \mathbf{a}(\tau_k)$ . It is easy to verify that  $\mathcal{A}_{1D}$  is centrally symmetric around the origin, and consequently it induces an atomic norm over  $\mathbb{C}^n$ , as defined in (2) and (3). It is worth noting that minimizing the atomic norm of  $\mathbf{x}$  is equivalent to minimizing the total variation of  $x(t)$ , and both viewpoints are used frequently in the literature.

Remarkably, this atomic norm admits an equivalent semidefinite program (SDP) characterization, thanks to the

Carathéodory–Fejér–Pisarenko decomposition [26]:

$$\|\mathbf{x}\|_{\mathcal{A}} = \inf_{\substack{\mathbf{u} \in \mathbb{C}^n \\ t > 0}} \left\{ \frac{1}{2n} \text{Tr}(\text{toep}(\mathbf{u})) + \frac{1}{2}t : \begin{bmatrix} \text{toep}(\mathbf{u}) & \mathbf{x} \\ \mathbf{x}^H & t \end{bmatrix} \succeq 0 \right\}. \quad (12)$$

Contrary to its abstract definition in (2), this reformulation (12) provides a tractable approach to *compute* the quantity  $\|\mathbf{x}\|_{\mathcal{A}}$ , which can be accomplished using generic off-the-shelf convex solvers [27].

#### B. Duality and Atomic Decomposition

The Lagrangian duality theory marks an important aspect in understanding the atomic norms. The study of the interactions between the primal atomic norm program and its Lagrange dual program grants a useful understanding of the properties of the optimal solutions, among other things [28].

The Lagrange dual problem associated with the atomic norm minimization (2) reads [11]

$$\max_{\mathbf{p}} \text{Re} \langle \mathbf{p}, \mathbf{x} \rangle \quad \text{subject to} \quad \|\mathbf{p}\|_{\mathcal{A}}^* \leq 1, \quad (13)$$

where the dual atomic norm  $\|\mathbf{p}\|_{\mathcal{A}}^*$  of a vector  $\mathbf{p} \in \mathbb{C}^n$  is defined with respect to the atomic set  $\mathcal{A}_{1D}$  as

$$\|\mathbf{p}\|_{\mathcal{A}}^* \triangleq \sup_{\mathbf{a} \in \mathcal{A}_{1D}} \text{Re} \langle \mathbf{a}, \mathbf{p} \rangle = \sup_{\tau \in [0, 1]} \underbrace{|\langle \mathbf{a}(\tau), \mathbf{p} \rangle|}_{P(\tau)}. \quad (14)$$

Since there is no inequality constraint in the primal problem (2), Slater's condition holds, and the optimal objective of the dual program (13) is equal to that of the primal program,  $\|\mathbf{x}\|_{\mathcal{A}}$ . The last equality of (14) suggests that the dual atomic norm can be interpreted as the supremum of the modulus of a complex trigonometric polynomial  $P(\tau) = \langle \mathbf{a}(\tau), \mathbf{p} \rangle = \sum_{\ell=0}^{n-1} p_\ell e^{-j2\pi\ell\tau}$  with coefficients given by the vector  $\mathbf{p}$ .

As a result, the constraint  $\|\mathbf{p}\|_{\mathcal{A}}^* \leq 1$  in (13) is equivalent to constraining the trigonometric polynomial  $P(\tau)$  to have modulus bounded by 1, which can be equivalently represented via semidefinite constraints by using the Bounded Real Lemma



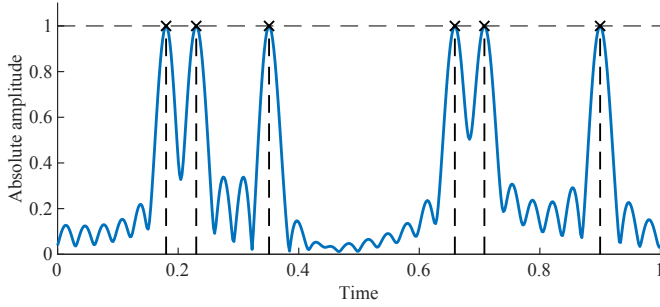


Fig. 4. Spike localization via localizing the peaks of the dual polynomial  $\hat{P}(\tau)$  (in blue) associated with the optimal solution  $\hat{\mathbf{p}}$  of the dual program (13) for a signal  $\mathbf{x}$  of length  $n = 33$  with 6 true spikes (in black).

[24], [25], [29], so that (13) is identical to the following SDP,

$$\begin{aligned} & \max_{\mathbf{p} \in \mathbb{C}^n, \mathbf{H} \in \mathbb{C}^{n \times n}} \operatorname{Re} \langle \mathbf{p}, \mathbf{x} \rangle \\ & \text{subject to} \quad \begin{bmatrix} \mathbf{H} & \mathbf{p} \\ \mathbf{p}^H & 1 \end{bmatrix} \succeq 0 \\ & \quad \sum_{i=1}^{n-k} H_{i,i+k} = \delta_k, \quad k = 0, \dots, n-1, \end{aligned}$$

where  $H_{i,j}$  is the  $(i, j)$ th entry of the matrix  $\mathbf{H}$ .

Another merit of the dual formulation is that the support set  $\mathcal{T}$  can be inferred from the optimal solution  $\hat{\mathbf{p}}$  to the dual problem (13), by examining the dual polynomial  $\hat{P}(\tau) = \langle \mathbf{a}(\tau), \hat{\mathbf{p}} \rangle$ . We identify the spikes as the locations of the extreme values of the modulus of  $\hat{P}(\tau)$ :

$$\hat{\mathcal{T}} = \left\{ \tau : |\hat{P}(\tau)| = 1 \right\}. \quad (15)$$

This approach is illustrated in Fig. 4 for a length-33 signal with 6 spikes, where all spikes are localized perfectly.

This offers an approach for super resolution that is drastically different from traditional methods, which rely heavily on the correctness of model order estimation. The dual polynomial approach, in contrast, does not require any prior knowledge on the model order, and can estimate the spikes with an infinitesimal precision.

### C. Exact Recovery Guarantees

So far, we have explained the algorithmic approach of atomic norm minimization for super resolution. A central question is to understand whether this convex relaxation is tight or not. More precisely, one would like to identify the conditions under which the estimated support  $\hat{\mathcal{T}}$  coincides with the true support  $\mathcal{T}$  of the signal  $\mathbf{x}$ , and correspondingly, the atomic decomposition coincides with the sparsest representation over the atomic set  $\mathcal{A}$ .

Such questions were extensively addressed in the context of  $\ell_1$  norm minimization, where the atomic set  $\mathcal{A}$  has a finite number of elements. The performance guarantees often depend on specific structural properties of  $\mathcal{A}$ , formalized in the notion of restricted isometry property (RIP) [30], or certain incoherence properties [31]. Unfortunately, these properties do not hold when considering a continuous dictionary such as

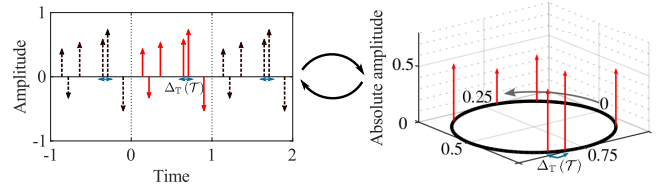


Fig. 5. A representation of the minimal wrap-around distance  $\Delta_{\mathbb{T}}(\mathcal{T})$  for a give set of spikes  $\mathcal{T}$ . The distance corresponds to the minimal gap between any element  $\tau \in \mathcal{T}$  and any distinct elements in the *aliased* set  $\mathcal{T} + \mathbb{Z}$ .

$\mathcal{A}_{1D}$ , since two atoms  $\mathbf{a}(\tau)$  and  $\mathbf{a}(\tau + \delta)$  can be more and more correlated with each other as their separation  $\delta$  tends to zero, leading to arbitrarily small RIP or coherence constants.

Nonetheless, one could ask for which class of signals the relaxation is tight. Intuitively, this depends on the separations between the spikes in  $\mathcal{T}$ . We introduce the minimal wrap-around distance  $\Delta_{\mathbb{T}}(\mathcal{T})$  over the torus  $\mathbb{T} = [0, 1)$  as

$$\Delta_{\mathbb{T}}(\mathcal{T}) \triangleq \inf_{\substack{\tau, \tau' \in \mathcal{T} \\ \tau \neq \tau'}} \min_{q \in \mathbb{Z}} |\tau - \tau' + q|.$$

This metric is illustrated by Fig. 5, and reflects the periodic behavior of the atom  $\mathbf{a}(\tau + p) = \mathbf{a}(\tau)$  for any integer  $p \in \mathbb{Z}$ . For instance, if  $\mathcal{T} = \{0.1, 0.9\}$ , then  $\Delta_{\mathbb{T}}(\mathcal{T}) = 0.2$ .

A surprising result, established by Candès and Fernandez-Granda in [11], is that for sufficiently large  $n$ , the atomic norm approach is tight, i.e.  $\hat{\mathcal{T}} = \mathcal{T}$ , as long as the separation condition  $\Delta_{\mathbb{T}}(\mathcal{T}) \geq \frac{4}{n-1}$  holds, regardless of the complex amplitudes of the spikes. Furthermore, this result is completely deterministic, and does not make any randomness assumptions on the signal. Later, this separation condition has been further improved by Fernandez-Granda [32] to  $\Delta_{\mathbb{T}}(\mathcal{T}) > \frac{2.52}{n-1}$ . Conversely, there exist some spike signals with  $\Delta_{\mathbb{T}}(\mathcal{T}) < \frac{2}{n-1}$  such that atomic norm minimization fails to resolve [33].

### D. Atomic Norm Denoising

In practice, the observations are corrupted by noise, and it is no longer possible to *exactly* recover the spike signal  $x(t)$ . This raises a natural question regarding the *robustness* of the estimate produced by atomic norm minimization methods. When the noise is additive and the observation  $\mathbf{z}$  obeys the noisy model (7), it has been proposed to estimate  $\mathbf{x}$  by searching around the observation  $\mathbf{z}$  for signals with small atomic norms [34]:

$$\min_{\mathbf{x}} \frac{1}{2} \|\mathbf{x} - \mathbf{z}\|_2^2 + \lambda \|\mathbf{x}\|_{\mathcal{A}}, \quad (16)$$

where  $\lambda > 0$  is a regularization parameter that draws a trade-off between the fidelity to the observations  $\mathbf{z}$  and the size of the atomic norm. This method, known as “atomic norm denoising”, can be interpreted as a generalization of the celebrated LASSO estimator [35].

When the noise vector  $\tilde{\mathbf{e}}$  is composed of i.i.d. complex Gaussian entries with zero mean and variance  $\sigma^2$ , the mean squared error (MSE) of the estimate  $\hat{\mathbf{x}}$  returned by (16) can

be bounded as [34]

$$\frac{1}{n} \|\widehat{\mathbf{x}} - \mathbf{x}\|_2^2 = O\left(\sigma \sqrt{\frac{\log n}{n}} \sum_{k=1}^r |c_k|\right)$$

with high probability by setting  $\lambda = \eta \sigma \sqrt{n \log n}$  for some constant  $\eta \in (1, \infty)$ . This error rate can be significantly improved when the spikes satisfy the separation condition  $\Delta_{\mathbb{T}}(\mathcal{T}) \geq \frac{4}{n-1}$ , where with high probability one has [36]

$$\frac{1}{n} \|\widehat{\mathbf{x}} - \mathbf{x}\|_2^2 = O\left(\sigma^2 \frac{r \log n}{n}\right).$$

This last error rate is near-optimal up to some logarithmic factor, since no estimator can achieve an MSE below the rate  $O\left(\sigma^2 \frac{r \log(n/r)}{n}\right)$  [36].

A more important performance criteria in super resolution concerns the stability of the support estimate  $\widehat{\mathcal{T}}$ , which has been studied in [36], [37], [38]. When the spikes satisfy the separation condition  $\Delta_{\mathbb{T}}(\mathcal{T}) > \frac{5.0018}{n-1}$ , and the complex amplitudes of the coefficients  $\{c_k\}_{1 \leq k \leq r}$  have approximately the same modulus, then it is established in [38] that the atomic decomposition of the output  $\widehat{\mathbf{x}}$  of (16) will be composed of the same number of spikes, i.e.  $|\widehat{\mathcal{T}}| = |\mathcal{T}| = r$  and that the estimated parameters satisfy

$$|c_k| |\widehat{\tau}_k - \tau_k| = O\left(\sigma \frac{\sqrt{\log n}}{n^{3/2}}\right), \quad |c_k - \widehat{c}_k| = O\left(\sigma \sqrt{\frac{\log n}{n}}\right)$$

with high probability.

Altogether, it can be seen that atomic norm denoising achieves near-optimal performance guarantees as long as the spikes are separated by a few times the Rayleigh limit. One might wonder if requiring a separation condition is necessary. Indeed, in the noise-free case, it makes atomic norm minimization seemingly inferior, since many methods do not require such a separation. However, when the spikes can take arbitrary complex amplitudes, some form of separation is unavoidable for *stable recovery* in noisy super resolution, no matter which method is used [39]. It is likely, though, the constants in the separation condition are subject to further improvements.

#### E. Can we discretize?

It may be worthwhile to pause and compare atomic norm minimization to other approaches based on convex optimization for super resolution, in particular,  $\ell_1$  minimization that is widely popular for high-resolution imaging and localization in the recent literature due to Compressed Sensing (CS) [40], [41].

The  $\ell_1$  norm can be seen as a discrete approximation of the atomic norm. Indeed, take the atomic set  $\mathcal{A}_{1D}$ , one can pick a desired resolution  $Q$  and discretize it into a finite set of atoms:

$$\mathcal{A}_{1D, \text{discrete}} = \left\{ e^{j\phi} \mathbf{a}\left(\frac{q}{Q}\right) : q = 0, \dots, Q-1, \phi \in [0, 2\pi) \right\},$$

and then perform  $\ell_1$  minimization over  $\mathcal{A}_{1D, \text{discrete}}$ . The convex hull of  $\mathcal{A}_{1D, \text{discrete}}$  approaches that of  $\mathcal{A}_{1D}$  as the discretization gets finer, which suggests the performance of  $\ell_1$  minimization over the discretized dictionary approaches that of atomic norm minimization asymptotically [42].

However, this discretization may come with several undesired consequences when the grid size  $Q$  is finite in practice. The theory of  $\ell_1$  minimization only provides guarantees when the spikes of  $x(t)$  lie exactly on the grid, which is unrealistic. In fact, there is always an inevitable mismatch [43], between the spikes represented in the discretized dictionary  $\mathcal{A}_{1D, \text{discrete}}$  and the true spikes, no matter how fine the grid is. Perfect recovery is not possible in this situation even in the absence of noise due to this mismatch. Furthermore, one can find signals whose representations in  $\mathcal{A}_{1D, \text{discrete}}$  are not compressible due to spectral leakage, and therefore are poorly recovered using  $\ell_1$  minimization, e.g. the recovery may contain many spurious spikes.

On the computational side, the time and memory complexities of  $\ell_1$  minimization rely on the size of the grid, which can become very expensive when the desired resolution is high. As we will illustrate later, tailored solvers make atomic norm minimization much more appealing computationally whose complexity does not scale with the grid size.

## IV. GENERALIZATIONS OF ATOMIC SETS

The tool of atomic norms can be extended easily to handle a wide range of scenarios in a unified manner, by properly adjusting the atomic set for signal decompositions, such as incorporating prior information, dealing with multi-dimensional settings and multiple measurement vectors, to illustrate a few.

### A. Atomic Set for Positive Spikes

In some applications, there exist additional information about the spikes, such as the coefficients of the spikes in (8) are positive, i.e.  $c_k > 0$ . Examples include neural spike sorting, fluorescence microscopy imaging, or covariance-based spectrum estimation for noncoherent sources [1].

In this case, the atomic set reduces to the moment curve  $\mathcal{A}_0$  in (10). The induced  $\|\mathbf{x}\|_{\mathcal{A}}$  is no longer a norm, since  $\mathcal{A}_0$  is not centrally symmetric, but nonetheless, similar SDP characterization still holds. To be specific, the dual program now becomes

$$\max_{\mathbf{p} \in \mathbb{C}^n} \operatorname{Re} \langle \mathbf{p}, \mathbf{x} \rangle \quad \text{subject to} \quad \sup_{\tau \in [0, 1]} \operatorname{Re} \langle \mathbf{a}(\tau), \mathbf{p} \rangle \leq 1,$$

where the constraint bounds the real part of the trigonometric polynomial  $P(\tau) = \langle \mathbf{a}(\tau), \mathbf{p} \rangle$ . Using the Fejér-Riesz Theorem [25], this can be equivalently represented as [44]:

$$\begin{aligned} & \max_{\mathbf{p} \in \mathbb{C}^n, \mathbf{H} \geq 0} \operatorname{Re} \langle \mathbf{p}, \mathbf{x} \rangle \\ & \text{subject to} \quad \sum_{i=1}^{n-k} H_{i, i+k} + p_k = \delta_k, \quad k = 0, \dots, n-1. \end{aligned}$$

It is long established [45], [46] that the spikes can be perfectly localized as long as  $r \leq \lfloor (n-1)/2 \rfloor$ , *without* requiring any separation between the spikes, as long as they are positive. The stability of this approach as well as the implications of nonnegative constraints for other atomic sets are further studied in [47], [48], [49], [50].

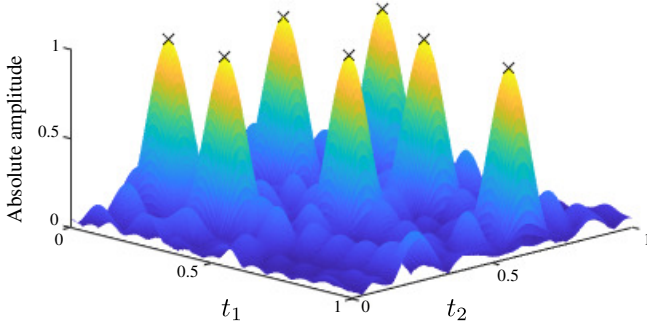


Fig. 6. An illustration of spike localization using the dual polynomial approach for two-dimensional spikes via atomic norm minimization. Here, we set  $n_1 = 12$ ,  $n_2 = 10$  and  $r = 7$ .

### B. Atomic Set for Multi-Dimensional Spikes

When the spikes reside in a multi-dimensional space, one can extend the one-dimensional model in a straightforward manner. Here, we illustrate the setup for the two-dimensional case, where each entry of the signal  $\mathbf{X}_{2D} \in \mathbb{C}^{n_1 \times n_2}$  can be expressed as a superposition of  $r$  complex sinusoids propagating in two directions:

$$\mathbf{X}_{2D} = \sum_{k=1}^r c_k \mathbf{a}_1(\tau_{1,k}) \mathbf{a}_2(\tau_{2,k})^\top, \quad (17)$$

where  $c_k$  and  $\boldsymbol{\tau}_k = [\tau_{1,k}, \tau_{2,k}]^\top \in [0, 1]^2$  are the complex amplitude and location of the  $k$ th spike, and  $\mathbf{a}_i(\tau)$  is given by (9) with the dimension parameter replaced by  $n_i$ ,  $i = 1, 2$ . It is natural to define the corresponding atomic set as [11], [51]

$$\mathcal{A}_{2D} = \left\{ e^{j\phi} \mathbf{a}_1(\tau_1) \mathbf{a}_2(\tau_2)^\top : \boldsymbol{\tau} \in [0, 1]^2, \phi \in [0, 2\pi) \right\},$$

and the atomic norm according to (2). To localize the spikes, one could similarly study the associated dual problem,

$$\max_{\mathbf{P} \in \mathbb{C}^{n_1 \times n_2}} \operatorname{Re} \langle \mathbf{P}, \mathbf{X} \rangle \quad \text{subject to } \|\mathbf{P}\|_{\mathcal{A}}^* \leq 1,$$

where the dual atomic norm can be reinterpreted as the supremum of a bivariate complex trigonometric polynomial  $P(\tau_1, \tau_2) = \langle \mathbf{P}, \mathbf{a}_1(\tau_1) \mathbf{a}_2(\tau_2)^\top \rangle$  with the matrix  $\mathbf{P}$  as its coefficients. Again, one can localize the spikes by examining the extremal points of the dual polynomial, which is illustrated in Fig. 6. Cautions need to be taken when attempting to solve the dual program in two or higher dimensions, since the Bounded Real Lemma [24], [25] does not hold anymore. Instead, a precise characterization requires solving a hierarchy of sum of squares relaxations, and fortunately in practice, the first level usually suffices [52], [24], [51].

The tightness of the atomic norm minimization approach is closely related to a separation condition analogous to the one-dimensional case [32]. Namely, the atomic decomposition is unique and exact, as soon as there exists a universal constant  $C > 0$  such that the set of spikes  $\mathcal{T} = \{\boldsymbol{\tau}_k\}_{1 \leq k \leq r}$  satisfies

$$\Delta_{\mathbb{T}^2}(\mathcal{T}) \triangleq \inf_{\substack{\boldsymbol{\tau}, \boldsymbol{\tau}' \in \mathcal{T} \\ \boldsymbol{\tau} \neq \boldsymbol{\tau}'}} \min_{\mathbf{q} \in \mathbb{Z}^2} \|\boldsymbol{\tau} - \boldsymbol{\tau}' + \mathbf{q}\|_{\infty} > \frac{C}{\min(n_1, n_2) - 1}.$$

Moreover, if the signal  $\mathbf{X}_{2D}$  is real-valued, choosing  $C = 4.76$  suffices.

### C. Atomic Set for Multiple Measurement Vectors

One can collect multiple snapshots of observations, where they share the same spike locations with varying coefficients. Consider  $L$  snapshots, stacked in a matrix,  $\mathbf{X}_{\text{MMV}} = [\mathbf{x}_1, \dots, \mathbf{x}_T]$ , which is expressed similarly to (8) as

$$\mathbf{X}_{\text{MMV}} = \sum_{k=1}^r \mathbf{a}(\tau_k) \mathbf{c}_k^\top, \quad (18)$$

where  $\mathbf{c}_k = [c_{1,k}, \dots, c_{L,k}] \in \mathbb{C}^T$  is the coefficient of the  $k$ th spike across the snapshots. Following the recipe of atomic norms, we define the atoms as

$$\mathbf{A}(\tau, \mathbf{b}) = \mathbf{a}(\tau) \mathbf{b}^\top,$$

where  $\tau \in [0, 1)$ ,  $\mathbf{b} \in \mathbb{C}^T$  with  $\|\mathbf{b}\|_2 = 1$ . The atomic set is defined as

$$\mathcal{A}_{\text{MMV}} = \{\mathbf{A}(\tau, \mathbf{b}) : \tau \in [0, 1), \|\mathbf{b}\|_2 = 1\}.$$

The atomic norm can be then defined following (2) which turns out sharing similar nice SDP characterizations for primal and dual formulations as for the single snapshot model [53]. The atomic norm  $\|\mathbf{X}_{\text{MMV}}\|_{\mathcal{A}}$  can be written equivalently as

$$\|\mathbf{X}_{\text{MMV}}\|_{\mathcal{A}} = \inf_{\substack{\mathbf{u} \in \mathbb{C}^n \\ \mathbf{W} \in \mathbb{C}^{T \times T}}} \left\{ \frac{1}{2n} \operatorname{Tr}(\operatorname{toep}(\mathbf{u})) + \frac{1}{2} \operatorname{Tr}(\mathbf{W}) : \begin{bmatrix} \operatorname{toep}(\mathbf{u}) & \mathbf{X}_{\text{MMV}} \\ \mathbf{X}_{\text{MMV}}^\top & \mathbf{W} \end{bmatrix} \succeq 0 \right\}. \quad (19)$$

A curious comparison can be drawn to the nuclear norm by noticing that one recovers the nuclear norm of  $\mathbf{X}_{\text{MMV}}$  by replacing the principal block  $\operatorname{toep}(\mathbf{u})$  in (19) with an arbitrary positive semidefinite matrix. The fact  $\operatorname{toep}(\mathbf{u})$  has significantly fewer degrees of freedom ( $n$  versus  $n^2$ ) is in parallel to that  $\mathbf{a}(\tau)$  has significantly fewer degrees of freedom than an arbitrary vector (1 versus  $n$ ).

One can determine the atomic decomposition and localize the spikes by resorting to the dual problem. Fig. 7 illustrated an example that multiple snapshots improve the performance of localization over the single snapshot case when the coefficients across snapshots exhibit some kind of diversity, e.g. generated with i.i.d. complex Gaussian entries.

## V. SUPER RESOLUTION BEYOND DENOISING

So far, we have seen that atomic norm minimization provides a means for super resolution via convex relaxation in additive Gaussian noise. The framework of convex optimization is quite versatile and can be extended to handle models when the measurements are partially observed, corrupted, contain interfering sources, or even come from unknown modulations. This is an important advantage over classical methods, as most of them cannot be extended easily to these variants of models.

### A. Compressed spectral sensing

CS [40], [41] have suggested that it is possible to recover a signal using a number of measurements that is proportional

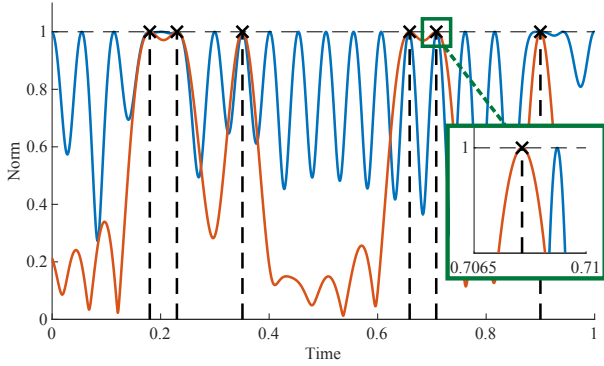


Fig. 7. The dual polynomial using multiple snapshots (in red) successfully localizes all the spikes while the one using a single snapshot (in blue) fails for the same spike signal. Here,  $r = 6$ ,  $n = 21$ , and  $L = 6$ .

to its degree of freedom, rather than its ambient dimension. Consider the problem where only a subset of entries of  $\mathbf{x}$  is observed,

$$\mathbf{y}_{CS} = \mathbf{A}_{CS}\mathbf{x},$$

where  $\mathbf{A}_{CS} \in \mathbb{C}^{m \times n}$ , and  $m \ll n$  representing compressive acquisition of the signal  $\mathbf{x}$ . The goal is to recover  $\mathbf{x}$  and its spectral content from  $\mathbf{y}_{CS} \in \mathbb{C}^m$ , the compressive measurements. This has applications in wideband spectrum sensing and cognitive radio [54], for example.

One can easily extend the framework of atomic norm minimization, and recover  $\mathbf{x}$  by solving the following program

$$\min_{\mathbf{x}} \|\mathbf{x}\|_{\mathcal{A}} \quad \text{subject to} \quad \mathbf{y}_{CS} = \mathbf{A}_{CS}\mathbf{x}.$$

When  $\mathbf{A}_{CS}$  is a partial observation matrix, namely, a subset of  $m$  entries of  $\mathbf{x}$  is observed uniformly at random, then  $\mathbf{x}$  can be perfectly recovered with high probability using  $m = O(\log^2 n + r \log r \log n)$  measurement as long as  $\mathbf{x}$  satisfies the separation condition with random signs of the coefficients  $c_k$ 's [16]. More generally, a broader class of measurement matrices  $\mathbf{A}_{CS}$  can be allowed where its rows are drawn independently from some isotropic and incoherent distribution [55], [56], and exact recovery is possible under the same separation condition using a number of measurements on the order of  $r$  up to some logarithmic factors.

### B. Demixing sinusoids and spikes

Due to sensor failures or malicious environments, the measurements are susceptible to corruptions that can take arbitrary magnitudes. To this end, consider the problem when the observations are contaminated by sparse outliers, where

$$\mathbf{y}_{\text{corrupt}} = \mathbf{x} + \mathbf{s}.$$

Here,  $\mathbf{s}$  is a sparse vector with the nonzero entries correspond to corruption. The goal is to decompose  $\mathbf{x}$  and  $\mathbf{s}$  from  $\mathbf{y}_{\text{corrupt}}$ , a problem intimately related to the uncertainty principle of signal decomposition in [57], [17] and sparse error correction in CS [58].

Leveraging low-dimensional structures in both  $\mathbf{x}$  and  $\mathbf{s}$ , we seek  $\mathbf{x}$  with a small atomic norm and  $\mathbf{s}$  with a small  $\ell_1$  norm

that satisfies the observation constraint [59]:

$$\min_{\mathbf{x}, \mathbf{s}} \|\mathbf{x}\|_{\mathcal{A}} + \lambda \|\mathbf{s}\|_1 \quad \text{subject to} \quad \mathbf{y}_{\text{corrupt}} = \mathbf{x} + \mathbf{s},$$

where  $\lambda > 0$  is some regularization parameter. As long as the sample size is sufficiently large [59], and the spikes satisfy the separation condition, among under mild conditions, then the above algorithm perfectly localizes the spikes with high probability, even when the corruption amounts to near a constant fraction of the measurements.

### C. Demixing interfering sources

A scenario of increasing interest is when the observation is composed of a mixture of responses from multiple exciting or transmitting sources, and the goal is to simultaneously separate and localize the sources at a high resolution. For example, an electrode probing the activities in a brain records firing patterns of a few neighboring neurons, each with a distinct PSF. For pedagogical reasons, let us consider a generalization of the model (6) with two interfering sources, where the observation is given as

$$\mathbf{y}_{\text{mix}} = \text{diag}(\mathbf{g}_1)\mathbf{x}_1 + \text{diag}(\mathbf{g}_2)\mathbf{x}_2,$$

where  $\mathbf{g}_1$  and  $\mathbf{g}_2$  correspond to the frequency-domain response of the PSFs, and  $\mathbf{x}_i = \sum_{k=1}^{r_i} c_{i,k} \mathbf{a}(\tau_{i,k})$ ,  $i = 1, 2$ . The goal is to separate and recover the spikes in both  $\mathbf{x}_1$  and  $\mathbf{x}_2$  from  $\mathbf{y}_{\text{mix}}$ , where  $\mathbf{g}_1$  and  $\mathbf{g}_2$  are assumed known.

Using atomic norm minimization, one seeks to recover both  $\mathbf{x}_1$  and  $\mathbf{x}_2$  simultaneously by minimizing the sum of their atomic norms [60]:

$$\begin{aligned} \min_{\mathbf{x}_1, \mathbf{x}_2} \quad & \|\mathbf{x}_1\|_{\mathcal{A}} + \lambda \|\mathbf{x}_2\|_{\mathcal{A}} \\ \text{subject to} \quad & \mathbf{y}_{\text{mix}} = \text{diag}(\mathbf{g}_1)\mathbf{x}_1 + \text{diag}(\mathbf{g}_2)\mathbf{x}_2, \end{aligned}$$

where  $\lambda > 0$  is some regularization parameter. Unlike the single source case, the success of demixing critically depends on how easy it is to tell two PSFs apart – the more similar  $\mathbf{g}_1$  and  $\mathbf{g}_2$  are, the harder it is to separate them. A random model can be used to generate dissimilar PSFs, namely, it is assumed the entries of  $\mathbf{g}_i$ 's are i.i.d. generated from a uniform distribution over the complex circle [60]. The algorithm then succeeds with high probability as long as the sample size is sufficiently large and the spikes within the same signal satisfy the separation condition [60], without requiring any separation for spikes coming from different sources.

### D. Blind super resolution

So far, all algorithms have assumed the PSF as known, which is a reasonable assumption for problems where one can design and calibrate the PSF a priori. In general, one might need to estimate the PSF at the same time, possibly due to the fact that the PSF may drift and needs to be calibrated on the fly during deployment. In this case, we need to revisit (6) and estimate simultaneously  $\mathbf{g}$  and  $\mathbf{x}$  from their bilinear measurements,

$$\mathbf{y}_{\text{BD}} = \text{diag}(\mathbf{g})\mathbf{x}.$$

This problem is terribly ill-posed, as the number of unknowns far exceeds the number of observations. One remedy is to



exploit additional structures of  $\mathbf{g}$ . For example, if  $\mathbf{g}$  lies in a known low-dimensional subspace  $\mathbf{B} = [\mathbf{b}_1, \dots, \mathbf{b}_n]^\top \in \mathbb{C}^{n \times d}$  with  $d \ll n$ , then the degrees of freedom of  $\mathbf{g}$  is greatly dropped, since one only needs to estimate the coefficient  $\mathbf{h} \in \mathbb{C}^d$  of  $\mathbf{g} = \mathbf{B}\mathbf{h}$  in that subspace, which is of much smaller dimension. Even such, the measurements  $\mathbf{y}_{\text{BD}}$  is still bilinear in  $\mathbf{h}$  and  $\mathbf{x}$ , and one cannot directly apply atomic norm minimization to  $\mathbf{x}$  as it does not lead to a convex program.

Interestingly, a lifting trick can be applied [61], which rewrites  $\mathbf{y}_{\text{BD}} = \mathcal{X}(\mathbf{Z})$  as linear measurements of a higher-dimensional object  $\mathbf{Z} = \mathbf{x}\mathbf{h}^\top \in \mathbb{C}^{n \times d}$  similar to (18):

$$y_{\text{BD},i} = \mathbf{b}_i^\top \mathbf{h} \mathbf{e}_i^\top \mathbf{x} = \langle \mathbf{x}\mathbf{h}^\top, \mathbf{e}_i \mathbf{b}_i^\top \rangle, \quad i = 1, \dots, n.$$

Consequently, one can apply atomic norm minimization to  $\mathbf{Z}$  with respect to (19), leading to the algorithm [61]:

$$\min_{\mathbf{Z}} \|\mathbf{Z}\|_{\mathcal{A}} \quad \text{subject to} \quad \mathbf{y}_{\text{BD}} = \mathcal{X}(\mathbf{Z}).$$

This approach succeeds with high probability as soon as the sample size is sufficiently large, the spikes are well-separated and the PSF satisfies certain incoherence properties. Moreover, it can be further extended to demixing a mixture of sources with unknown PSFs, where each PSF lies in a distinct subspace, see [62].

## VI. FASTER ALGORITHMS

While the SDP formulation is tractable, its computational complexity is prohibitive when solving large-dimension problems. Fortunately, it is possible to develop tailored algorithms that are significantly faster. For conciseness, we will discuss two approaches based on the Alternating Direction Method of Multipliers (ADMM) [34] and the Alternating Descent Conditional Gradient (ADCG) method [63].

### A. ADMM

The general principle of ADMM is to split the Lagrangian function of an optimization problem into a sum of separable sub-functions [64]. Each iteration of the algorithm consists in performing independent local minimization on each of those quantities, while ensuring that the feasibility constraints are always satisfied. The iterations run until both primal and dual residuals satisfy a pre-defined tolerance level.

We take atomic norm denoising (16) as an example, which, in light of (12), can be equivalently rewritten as

$$\begin{aligned} \min_{\mathbf{x}, \mathbf{u}, t} \quad & \frac{1}{2} \|\mathbf{x} - \mathbf{z}\|_2^2 + \frac{\lambda}{2} \left( \frac{1}{n} \text{Tr}(\text{toep}(\mathbf{u})) + t \right) \\ \text{subject to} \quad & \mathbf{S} = \begin{bmatrix} \text{toep}(\mathbf{u}) & \mathbf{x} \\ \mathbf{x}^\text{H} & t \end{bmatrix}, \mathbf{S} \succeq 0. \end{aligned}$$

The above program has been ‘‘augmented’’ by introducing an intermediate variable  $\mathbf{S}$  for the purpose of decoupling the positive semidefinite constraint on the matrix  $\mathbf{S}$  from the linear

---

### Algorithm 1 ADMM for atomic norm denoising [34]

---

**Input:** Observation  $\mathbf{z}$ ; Parameters  $\lambda, \rho > 0$ ;

Initialize  $j = 0$ , and  $\Sigma_0, \mathbf{S}_0$  to zero matrices

**repeat** until stopping criteria

$$(\mathbf{x}_{j+1}, \mathbf{u}_{j+1}, t_{j+1}) \leftarrow \underset{\mathbf{c}, \mathbf{u}, t}{\text{argmin}} \mathcal{L}(\mathbf{x}, \mathbf{u}, t, \Sigma_j, \mathbf{S}_j);$$

$$\mathbf{S}_{j+1} \leftarrow \underset{\mathbf{S} \succeq 0}{\text{argmin}} \mathcal{L}(\mathbf{x}_{j+1}, \mathbf{u}_{j+1}, t_{j+1}, \Sigma_j, \mathbf{S});$$

$$\Sigma_{j+1} \leftarrow \Sigma_j + \rho \left( \mathbf{S}_{j+1} - \begin{bmatrix} \text{toep}(\mathbf{u}_{j+1}) & \mathbf{x}_{j+1} \\ \mathbf{x}_{j+1}^\text{H} & t_{j+1} \end{bmatrix} \right);$$

$$j \leftarrow j + 1;$$

**Output:**  $\mathbf{x}_j$

---

constraints on its structure. The augmented Lagrangian  $\mathcal{L}$  writes

$$\begin{aligned} \mathcal{L}(\mathbf{x}, \mathbf{u}, t, \Sigma, \mathbf{S}) = & \frac{1}{2} \|\mathbf{x} - \mathbf{z}\|_2^2 + \frac{\lambda}{2} \left( \frac{1}{n} \text{Tr}(\text{toep}(\mathbf{u})) + t \right) \\ & + \left\langle \Sigma, \mathbf{S} - \begin{bmatrix} \text{toep}(\mathbf{u}) & \mathbf{x} \\ \mathbf{x}^\text{H} & t \end{bmatrix} \right\rangle \\ & + \frac{\rho}{2} \left\| \mathbf{S} - \begin{bmatrix} \text{toep}(\mathbf{u}) & \mathbf{x} \\ \mathbf{x}^\text{H} & t \end{bmatrix} \right\|_{\text{F}}^2, \end{aligned}$$

where  $\mathbf{S}$  and  $\Sigma$  are  $(n+1)$ -dimensional Hermitian matrices, and  $\rho > 0$  is a regularization parameter. The successive update steps to minimize the augmented Lagrangian are given in Alg. 1. Closed-form solutions can be found for the first update step, yielding a very efficient implementation. The second update is the most costly part where a projection over the set of positive semidefinite Hermitian matrices has to be computed, which is typically achieved using power methods.

### B. ADCG

The ADCG method [63] is an acceleration of the conditional gradient method, also known as Frank-Wolfe, to solve sparse inverse problems over continuous dictionaries with general convex loss functions. Taking the constrained form of atomic norm denoising as an example, ADCG aims to solve the following problem:

$$\min_{\mathbf{x}} \frac{1}{2} \|\mathbf{x} - \mathbf{z}\|_2^2 \quad \text{subject to} \quad \|\mathbf{x}\|_{\mathcal{A}} \leq \eta,$$

where  $\eta > 0$  is a regularization parameter. Given an atomic set  $\mathcal{A}_{\text{1D}}$ , it directly estimates the support and corresponding coefficients  $(\mathcal{T}, \mathbf{c})$ .

The detailed procedure of ADCG is given in Alg. 2. In the  $j$ th iteration, denote  $\mathcal{A}(\mathcal{T}_j)$  as the matrix whose columns are the atoms  $\mathbf{a}(\tau)$  with  $\tau \in \mathcal{T}_j$ . ADCG starts by adding a spike to the estimated support  $\mathcal{T}_j$  that maximally correlates with the residual of the current estimate,  $\mathcal{A}(\mathcal{T}_j)\mathbf{c}_j - \mathbf{z}$ . Then ADCG iterates between coefficients update via  $\ell_1$  minimization, support pruning, and local refinement of the support. The last step leverages the fact that  $\mathbf{a}(\tau)$  is differentiable with respect to  $\tau$ , and a simple local search via gradient descent allows one to adjust the support to further reduce the loss function. The main computational benefits of ADCG are the absence of

**Algorithm 2** ADCG for atomic norm denoising [63]

**Input:** Observation  $\mathbf{z}$ ; Parameter  $\eta > 0$ ;  
 Initialize  $\mathcal{T}_0$  to an empty set,  $\mathbf{c}_0$  to  $\mathbf{0}$ , and  $j = 0$ ;  
**repeat** until stopping criteria  
 Localize the next spike:

$$\tau_{j+1} \in \operatorname{argmax}_{\tau \in [0,1]} |\langle \mathbf{a}(\tau), \mathcal{A}(\mathcal{T}_j)\mathbf{c}_j - \mathbf{z} \rangle|;$$

Update support:  $\mathcal{T}_{j+1} \leftarrow \mathcal{T}_j \cup \{\tau_{j+1}\}$ ;

Refinement: **repeat**

1) Update the amplitudes:

$$\mathbf{c}_{j+1} \leftarrow \operatorname{argmin}_{\|\mathbf{c}\|_1 \leq \eta} \frac{1}{2} \|\mathcal{A}(\mathcal{T}_{j+1})\mathbf{c} - \mathbf{z}\|_2^2;$$

2) Prune support:  $\mathcal{T}_{j+1} \leftarrow \operatorname{support}(\mathbf{c}_{j+1})$ ;

3) Locally improve  $\mathcal{T}_{j+1}$  by performing local descent with respect to  $\tau$ ;

$j \leftarrow j + 1$ ;

**Output:**  $(\mathcal{T}_j, \mathbf{c}_j)$  and  $\mathbf{x}_j = \mathcal{A}(\mathcal{T}_j)\mathbf{c}_j$ .

semidefinite constraints and small memory footprints, making it highly suitable for large-scale implementations.

## VII. SUPER-RESOLUTION IMAGING IN SINGLE-MOLECULE FLUORESCENCE MICROSCOPY

The development of super-resolution fluorescence microscopy, which has been awarded the 2014 Nobel prize in Chemistry, has enabled noninvasive imaging of complex biological processes at the nanometer scale, and is considered to fundamentally impact biological science and medicine. To date, a partial list of super-resolution fluorescence microscopy technologies includes PALM [65], STORM [66], and fPALM [67] that share a similar imaging principle. By employing photoswitchable fluorescent molecules, the imaging process is divided into many frames, where in each frame, a *sparse* number of fluorophores (point sources) are randomly activated, localized at a resolution below the diffraction limit, and deactivated. The final image is thus obtained by superimposing the localization outcomes of all the frames. Therefore, the high spatial resolution is achieved by sacrificing the temporal resolution. To speed up the imaging process and improve the temporal resolution, it is desirable to develop localization algorithms that can handle higher emitter density.

The imaging principle can be extended to reconstruct a 3-D object from 2-D image frames [68]. One way is to introduce a cylindrical lens to modulate the ellipticity of the PSF based on the depth of the fluorescent object, which can be modeled as a Gaussian pulse with varying ellipticity along the  $x$  and  $y$  directions,

$$g(x, y|z) = \frac{1}{2\pi\sigma_x(z)\sigma_y(z)} \exp\left(-\frac{x^2}{2\sigma_x(z)^2} + \frac{y^2}{2\sigma_y(z)^2}\right),$$

where  $\sigma_x(z)$  and  $\sigma_y(z)$  are calibrated in advance. As illustrated in Fig. 8, the 3-D scene of point sources  $x(t)$  undergoes a low-pass convolution, pixelization, and then Poisson noise until one collects the discrete measurements  $\mathbf{z}$ , which can be modeled

by a likelihood function  $p(\mathbf{z}|x(t))$ . The goal is to recover  $x(t)$  from  $\mathbf{z}$  as accurately as possible.

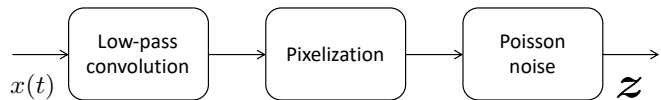


Fig. 8. The mathematical model of imaging in three-dimensional fluorescence microscopy.

Sparsity-promoting optimization-based recovery methods are perfect candidates to speed up the process and quality of super-resolution imaging. Early efforts include CSSTORM [69], which are based on  $\ell_1$  minimization by directly discretizing the parameter space. More recently, TVSTORM [70] is proposed as a tailored algorithm for 3-D image reconstruction by adapting ADCG to solve a penalized maximum likelihood estimation with atomic norm regularization, which outperforms CSSTORM both in terms of computational time and reconstruction quality. Fig. 9 (a) shows the diffraction-limited imaging using conventional microscopy; in contrast, the 3-D super-resolution image reconstructed using TVSTORM in Fig. 9 (b) is much clearer, where the structure of 3D microtubules can be well resolved with the axial coordinate represented in different colors. Fig. 9 (c) and (d) compare the reconstruction quality of a zoom-in region between TVSTORM and CSSTORM, where TVSTORM provides a visually more smooth reconstruction of the line structures in microtubules, since it has a higher detection rate and a lower false discovery rate than CSSTORM.

## VIII. FINAL REMARKS

In this paper, we presented an overview on how to leverage sparsity for continuous parameter estimation via the mathematical concept of atomic norms, which can be regarded as a generalization of the principle of  $\ell_1$  norms for discrete model selection. We showcased its application in super resolution from low-pass observations in single-molecule fluorescence microscopy. The appeals of the atomic norm approach come from its elegant mathematical framework, strong performance guarantees, and promises to scalable numerical solvers.

The atomic norm is only one of many possible approaches to exploit sparsity over the continuum. Another competitive approach is structured low-rank matrix optimization [71], [72], [73]; see [44] for its connections and comparisons with the atomic norm approach. As a topic still under development, open problems abound for both theory and practical performance of optimization-based super-resolution in general. In particular, it is of great interest to study the connections between traditional approaches (Prony, MUSIC, and so on) and optimization-based approaches such as atomic norm minimization and nuclear norm minimization. Such connections have already been realized in the early works of Fuchs [74], where he provided an optimization interpretation of the Pisarenko method [75]. Another recent work [76] provided an optimization view to the MUSIC algorithm. It is hopeful that a confluence of past and current ideas will likely deepen our understandings and lead to further algorithmic improvements.

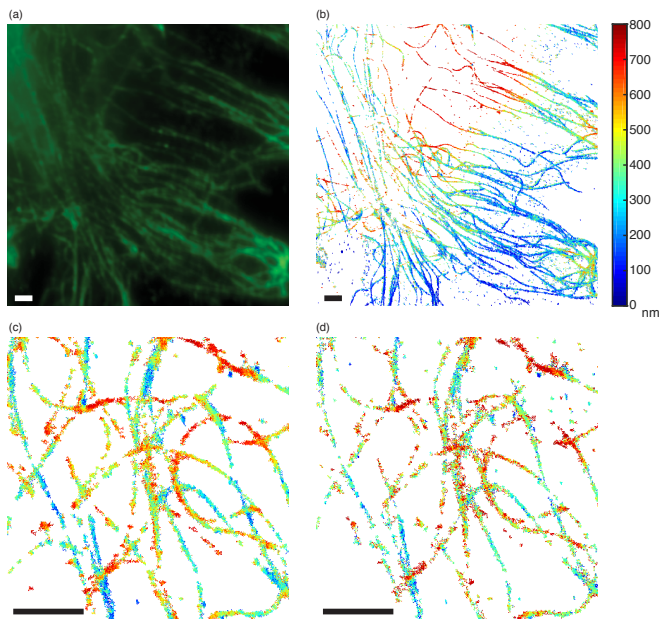


Fig. 9. (a) Diffraction-limited imaging of microtubules using conventional microscopy and (b) super-resolution 3D image reconstruction using TVSTORM. Comparison of reconstruction quality between (c) TVSTORM and (d) CSSTORM (bar:  $1.5 \mu\text{m}$ ). Image credit: [70].

## REFERENCES

- [1] P. Stoica and R. L. Moses, *Introduction to spectral analysis*. New Jersey: Prentice Hall, 1997, vol. 1.
- [2] S. M. Kay and S. L. Marple, "Spectrum analysis—a modern perspective," *Proceedings of the IEEE*, vol. 69, no. 11, pp. 1380–1419, 1981.
- [3] R. Prony, "Essai experimental et analytique," *J. de l'Ecole Polytechnique (Paris)*, vol. 1, no. 2, pp. 24–76, 1795.
- [4] R. Kumaresan, D. Tufts, and L. L. Scharf, "A prony method for noisy data: Choosing the signal components and selecting the order in exponential signal models," *Proceedings of the IEEE*, vol. 72, no. 2, pp. 230–233, 1984.
- [5] R. Schmidt, "Multiple emitter location and signal parameter estimation," *IEEE Transactions on Antennas and Propagation*, vol. 34, no. 3, pp. 276–280, 1986.
- [6] R. Roy and T. Kailath, "ESPRIT-estimation of signal parameters via rotational invariance techniques," *IEEE Transactions on Acoustics, Speech and Signal Processing*, vol. 37, no. 7, pp. 984–995, Jul 1989.
- [7] Y. Hua and T. K. Sarkar, "Matrix pencil method for estimating parameters of exponentially damped/undamped sinusoids in noise," *IEEE Transactions on Acoustics, Speech and Signal Processing*, vol. 38, no. 5, pp. 814–824, may 1990.
- [8] P. Stoica, R. L. Moses, B. Friedlander, and T. Soderstrom, "Maximum likelihood estimation of the parameters of multiple sinusoids from noisy measurements," *IEEE Transactions on Acoustics, Speech, and Signal Processing*, vol. 37, no. 3, pp. 378–392, 1989.
- [9] M. P. Clark and L. L. Scharf, "Two-dimensional modal analysis based on maximum likelihood," *IEEE Transactions on Signal Processing*, vol. 42, no. 6, pp. 1443–1452, 1994.
- [10] M. Born and E. Wolf, *Principles of optics: electromagnetic theory of propagation, interference and diffraction of light*. Cambridge university press, 1999.
- [11] E. J. Candès and C. Fernandez-Granda, "Towards a mathematical theory of super-resolution," *Communications on Pure and Applied Mathematics*, vol. 67, no. 6, pp. 906–956, 2014.
- [12] B. Huang, M. Bates, and X. Zhuang, "Super-resolution fluorescence microscopy," *Annual review of biochemistry*, vol. 78, pp. 993–1016, 2009.
- [13] V. Chandrasekaran, B. Recht, P. A. Parrilo, and A. S. Willsky, "The convex geometry of linear inverse problems," *Foundations of Computational Mathematics*, vol. 12, no. 6, pp. 805–849, 2012.
- [14] S. Chen, D. L. Donoho, and M. A. Saunders, "Atomic decomposition by basis pursuit," *SIAM Review*, vol. 43, no. 1, pp. 129–159, 2001.
- [15] B. Recht, M. Fazel, and P. A. Parrilo, "Guaranteed minimum-rank solutions of linear matrix equations via nuclear norm minimization," *SIAM review*, vol. 52, no. 3, pp. 471–501, 2010.
- [16] G. Tang, B. N. Bhaskar, P. Shah, and B. Recht, "Compressed sensing off the grid," *IEEE transactions on information theory*, vol. 59, no. 11, pp. 7465–7490, 2013.
- [17] D. Donoho and X. Huo, "Uncertainty principles and ideal atomic decomposition," *IEEE Transactions on Information Theory*, vol. 47, no. 7, pp. 2845–2862, November 2001.
- [18] Y. Chen and Y. Chi, "Harnessing structures in big data via guaranteed low-rank matrix estimation: Recent theory and fast algorithms via convex and nonconvex optimization," *IEEE Signal Processing Magazine*, vol. 35, no. 4, pp. 14–31, 2018.
- [19] E. J. Candès, J. K. Romberg, and T. Tao, "Stable signal recovery from incomplete and inaccurate measurements," *Communications on Pure and Applied Mathematics*, vol. 59, no. 8, pp. 1207–1223, 2006.
- [20] D. Donoho, "For most large underdetermined systems of linear equations the minimal  $l_1$ -norm solution is also the sparsest solution," *Comm. Pure and Applied Math.*, vol. 59, no. 6, pp. 797–829, 2006.
- [21] C. Carathéodory, "Über den variabilitätsbereich der fourier'schen konstanten von positiven harmonischen funktionen," *Rendiconti Del Circolo Matematico di Palermo (1884-1940)*, vol. 32, no. 1, pp. 193–217, 1911.
- [22] S. Foucart and H. Rauhut, *A Mathematical Introduction to Compressive Sensing*. Springer Science & Business Media, 2013.
- [23] R. Sanyal, F. Sottile, and B. Sturmfels, "Orbitopes," *Mathematika*, vol. 57, no. 2, pp. 275–314, 2011.
- [24] J.-B. Lasserre, *Moments, positive polynomials and their applications*. World Scientific, 2010, vol. 1.
- [25] B. Dumitrescu, *Positive trigonometric polynomials and signal processing applications*. Springer, 2007.
- [26] T. T. Georgiou, "The carathéodory–fejér–pisarenko decomposition and its multivariable counterpart," *IEEE transactions on automatic control*, vol. 52, no. 2, pp. 212–228, 2007.
- [27] M. Grant and S. Boyd, "Cvx: Matlab software for disciplined convex programming."
- [28] S. Boyd and L. Vandenberghe, *Convex optimization*. Cambridge university press, 2009.
- [29] O. Teke and P. P. Vaidyanathan, "On the role of the bounded lemma in the SDP formulation of atomic norm problems," *IEEE Signal Processing Letters*, vol. 24, no. 7, pp. 972–976, 2017.
- [30] E. J. Candès, "The restricted isometry property and its implications for compressed sensing," *Comptes Rendus Mathématique*, vol. 346, no. 9, pp. 589–592, 2008.
- [31] J. A. Tropp and A. C. Gilbert, "Signal recovery from random measurements via orthogonal matching pursuit," *IEEE Transactions on Information Theory*, vol. 53, no. 12, pp. 4655–4666, 2007.
- [32] C. Fernandez-Granda, "Super-resolution of point sources via convex programming," *Information and Inference*, vol. 5, no. 3, pp. 251–303, sep 2016.
- [33] M. Ferreira Da Costa and W. Dai, "A tight converse to the spectral resolution limit via convex programming," in *2018 IEEE International Symposium on Information Theory (ISIT)*, Jun. 2018, pp. 901–905.
- [34] B. N. Bhaskar, G. Tang, and B. Recht, "Atomic norm denoising with applications to line spectral estimation," *IEEE Transactions on Signal Processing*, vol. 61, no. 23, pp. 5987–5999, 2013.
- [35] R. Tibshirani, "Regression shrinkage and selection via the lasso," *Journal of the Royal Statistical Society. Series B (Methodological)*, vol. 58, no. 1, pp. 267–288, 1996.
- [36] G. Tang, B. N. Bhaskar, and B. Recht, "Near minimax line spectral estimation," *IEEE Transactions on Information Theory*, vol. 61, no. 1, pp. 499–512, 2015.
- [37] C. Fernandez-Granda, "Support detection in super-resolution," in *Proceedings of the 10th International Conference on Sampling Theory and Applications (SampTA 2013)*, 2013, pp. 145–148.
- [38] Q. Li and G. Tang, "Approximate support recovery of atomic line spectral estimation: A tale of resolution and precision," *Applied and Computational Harmonic Analysis*, 2018.
- [39] A. Moitra, "Super-resolution, extremal functions and the condition number of vandermonde matrices," in *Proceedings of the forty-seventh annual ACM symposium on Theory of computing*. ACM, 2015, pp. 821–830.
- [40] E. J. Candès and T. Tao, "Near-optimal signal recovery from random projections: Universal encoding strategies?" *IEEE Trans. Info. Theory*, vol. 52, no. 12, pp. 5406 – 5424, Dec. 2006.
- [41] D. L. Donoho, "Compressed sensing," *IEEE Transactions on Information Theory*, vol. 52, no. 4, pp. 1289 – 1306, Apr. 2006.

- [42] G. Tang, B. N. Bhaskar, and B. Recht, "Sparse recovery over continuous dictionaries-just discretize," in *2013 Asilomar Conference on Signals, Systems and Computers*, Nov 2013, pp. 1043–1047.
- [43] Y. Chi, L. Scharf, A. Pezeshki, and A. Calderbank, "Sensitivity to basis mismatch in compressed sensing," *IEEE Transactions on Signal Processing*, vol. 59, no. 5, pp. 2182–2195, May 2011.
- [44] Y. Chi, "Convex relaxations of spectral sparsity for robust super-resolution and line spectrum estimation," in *Wavelets and Sparsity XVII*, vol. 10394. International Society for Optics and Photonics, 2017, p. 103941G.
- [45] D. L. Donoho and J. Tanner, "Sparse nonnegative solution of underdetermined linear equations by linear programming," *Proceedings of the National Academy of Sciences of the United States of America*, vol. 102, no. 27, pp. 9446–9451, 2005.
- [46] J.-J. Fuchs, "Sparsity and uniqueness for some specific under-determined linear systems," in *Proceedings of IEEE International Conference on Acoustics, Speech, and Signal Processing*, vol. 5. IEEE, 2005, pp. v–729.
- [47] Q. Denoyelle, V. Duval, and G. Peyré, "Support recovery for sparse super-resolution of positive measures," *Journal of Fourier Analysis and Applications*, vol. 23, no. 5, pp. 1153–1194, 2017.
- [48] G. Schiebinger, E. Robeva, and B. Recht, "Superresolution without separation," *Information and Inference: A Journal of the IMA*, vol. 7, no. 1, pp. 1–30, 2017.
- [49] A. Eftekhari, J. Tanner, A. Thompson, B. Toader, and H. Tyagi, "Sparse non-negative super-resolution-simplified and stabilised," *arXiv preprint arXiv:1804.01490*, 2018.
- [50] V. I. Morgenshtern and E. J. Candes, "Super-resolution of positive sources: The discrete setup," *SIAM Journal on Imaging Sciences*, vol. 9, no. 1, pp. 412–444, 2016.
- [51] Y. Chi and Y. Chen, "Compressive two-dimensional harmonic retrieval via atomic norm minimization," *IEEE Transactions on Signal Processing*, vol. 63, no. 4, pp. 1030–1042, 2015.
- [52] W. Xu, J.-F. Cai, K. V. Mishra, M. Cho, and A. Kruger, "Precise semidefinite programming formulation of atomic norm minimization for recovering  $d$ -dimensional ( $d \geq 2$ ) off-the-grid frequencies," in *Information Theory and Applications Workshop (ITA), 2014*. IEEE, 2014, pp. 1–4.
- [53] Y. Li and Y. Chi, "Off-the-grid line spectrum denoising and estimation with multiple measurement vectors," *Signal Processing, IEEE Transactions on*, vol. 64, no. 5, pp. 1257–1269.
- [54] Z. Tian and G. B. Giannakis, "Compressed sensing for wideband cognitive radios," in *2007 IEEE International Conference on Acoustics, Speech and Signal Processing*, vol. 4. IEEE, 2007, pp. IV–1357.
- [55] E. J. Candes and Y. Plan, "A probabilistic and ripples theory of compressed sensing," *Information Theory, IEEE Transactions on*, vol. 57, no. 11, pp. 7235–7254, 2011.
- [56] R. Heckel and M. Soltanolkotabi, "Generalized line spectral estimation via convex optimization," *IEEE Transactions on Information Theory*, vol. 64, no. 6, pp. 4001–4023, 2018.
- [57] D. L. Donoho and P. B. Stark, "Uncertainty principles and signal recovery," *SIAM Journal on Applied Mathematics*, vol. 49, no. 3, pp. 906–931, 1989.
- [58] X. Li, "Compressed sensing and matrix completion with constant proportion of corruptions," *Constructive Approximation*, vol. 37, pp. 73–99, 2013.
- [59] C. Fernandez-Granda, G. Tang, X. Wang, and L. Zheng, "Demixing sines and spikes: Robust spectral super-resolution in the presence of outliers," *Information and Inference: A Journal of the IMA*, vol. 7, no. 1, pp. 105–168, 2017.
- [60] Y. Li and Y. Chi, "Stable separation and super-resolution of mixture models," *Applied and Computational Harmonic Analysis*, vol. 46, no. 1, pp. 1–39, 2019.
- [61] Y. Chi, "Guaranteed blind sparse spikes deconvolution via lifting and convex optimization," *IEEE Journal of Selected Topics in Signal Processing*, vol. 10, no. 4, pp. 782–794, 2016.
- [62] D. Yang, G. Tang, and M. B. Wakin, "Super-resolution of complex exponentials from modulations with unknown waveforms," *IEEE Transactions on Information Theory*, vol. 62, no. 10, pp. 5809–5830, 2016.
- [63] N. Boyd, G. Schiebinger, and B. Recht, "The alternating descent conditional gradient method for sparse inverse problems," *SIAM Journal on Optimization*, vol. 27, no. 2, pp. 616–639, 2017.
- [64] S. Boyd, N. Parikh, E. Chu, B. Peleato, and J. Eckstein, "Distributed Optimization and Statistical Learning via the Alternating Direction Method of Multipliers," *Foundations and Trends in Machine Learning*, vol. 3, no. 1, pp. 1–122, 2010.
- [65] E. Betzig, G. H. Patterson, R. Sougrat, O. W. Lindwasser, S. Olenych, J. S. Bonifacio, M. W. Davidson, J. Lippincott-Schwartz, and H. F. Hess, "Imaging intracellular fluorescent proteins at nanometer resolution," *Science*, vol. 313, no. 5793, pp. 1642–1645, 2006.
- [66] M. J. Rust, M. Bates, and X. Zhuang, "Sub-diffraction-limit imaging by stochastic optical reconstruction microscopy (storm)," *Nature methods*, vol. 3, no. 10, pp. 793–796, 2006.
- [67] S. T. Hess, T. P. Girirajan, and M. D. Mason, "Ultra-high resolution imaging by fluorescence photoactivation localization microscopy," *Biophysical Journal*, vol. 91, no. 11, pp. 4258–4272, 2006.
- [68] B. Huang, W. Wang, M. Bates, and X. Zhuang, "Three-dimensional super-resolution imaging by stochastic optical reconstruction microscopy," *Science*, vol. 319, no. 5864, pp. 810–813, February 2008.
- [69] L. Zhu, W. Zhang, D. Elnatan, and B. Huang, "Faster STORM using compressed sensing," *Nature methods*, vol. 9, no. 7, p. 721, 2012.
- [70] J. Huang, M. Sun, J. Ma, and Y. Chi, "Super-resolution image reconstruction for high-density three-dimensional single-molecule microscopy," *IEEE Transactions on Computational Imaging*, vol. 3, no. 4, pp. 763–773, 2017.
- [71] Y. Chen and Y. Chi, "Robust spectral compressed sensing via structured matrix completion," *Information Theory, IEEE Transactions on*, vol. 60, no. 10, pp. 6576–6601, Oct 2014.
- [72] K. H. Jin, D. Lee, and J. C. Ye, "A general framework for compressed sensing and parallel mri using annihilating filter based low-rank hankel matrix," *IEEE Transactions on Computational Imaging*, vol. 2, no. 4, pp. 480–495, 2016.
- [73] G. Ongie, S. Biswas, and M. Jacob, "Convex recovery of continuous domain piecewise constant images from nonuniform fourier samples," *IEEE Transactions on Signal Processing*, vol. 66, no. 1, pp. 236–250.
- [74] J.-J. Fuchs, "Extension of the Pisarenko method to sparse linear arrays," *IEEE Transactions on Signal Processing*, vol. 45, no. 10, pp. 2413–2421, 1997.
- [75] V. F. Pisarenko, "The retrieval of harmonics from a covariance function," *Geophysical Journal International*, vol. 33, no. 3, pp. 347–366, 1973.
- [76] S. Li, H. Mansour, and M. B. Wakin, "An optimization view of music and its extension to missing data," *arXiv preprint arXiv:1806.03511*, 2018.

PLACE  
PHOTO  
HERE

**Yuejie Chi** (S'09-M'12-SM'17) received the Ph.D. degree in Electrical Engineering from Princeton University in 2012, and the B.E. (Hon.) degree in Electrical Engineering from Tsinghua University, Beijing, China, in 2007. She was with The Ohio State University from 2012 to 2017. Since 2018, she is an Associate Professor with the department of Electrical and Computer Engineering at Carnegie Mellon University, where she holds the Robert E. Doherty Early Career Professorship. Her research interests include signal processing, statistical inference, machine learning, large-scale optimization, and their applications in data science, inverse problems, imaging, and sensing systems.

She is a recipient of the IEEE Signal Processing Society Young Author Best Paper Award and the Best Paper Award at the IEEE International Conference on Acoustics, Speech, and Signal Processing (ICASSP). She received the NSF CAREER Award, AFOSR and ONR Young Investigator Program Awards, Ralph E. Powe Junior Faculty Enhancement Award, and Google Faculty Research Award. She has served as an Elected Member of the SPTM, SAM and MLSP Technical Committees of the IEEE Signal Processing Society. She is also an Associate Editor of IEEE Trans. on Signal Processing.

PLACE  
PHOTO  
HERE

**Maxime Ferreira Da Costa** (S'14-M'18) received the Ph.D. degree in Electrical and Electronic Engineering from Imperial College London, UK, in 2018. He has been awarded the M.Sc in Signal Processing from Imperial College London in 2012, and the Diplôme d'Ingénieur from Supélec, France, the same year. Since October 2018, he is a Research Associate with the department of Electrical and Computer Engineering at Carnegie Mellon University. His research focuses on mathematical signal processing, inverse problems and optimization. In 2018, he was shortlisted among the finalists for the Jack Keil Wolf Student Paper Award at the IEEE International Symposium on Information Theory (ISIT).